Textures and Microstructures, Vol. 33, pp. 343–355
Reprints available directly from the publisher
Photocopying permitted by license only

OPTIMIZATION OF TEXTURE MEASUREMENTS. I. METHOD: OPTIMAL GRID PARAMETER

V. LUZIN

Joint Institute for Nuclear Research, Frank Laboratory of Neutron Physics
141980 Dubna, Moscow Region, Russia

(Received 1 October 1997)

In texture experiments one always measures a sample with some constrained number of grains N (see the discussion in Bunge (1996). *Proc. of Workshop "Math. Methods of Texture Analysis"*, *Textures and Microstructures* **25**, 71–108). It is clear that the orientation distribution function (ODF) and pole figures (PFs) measured for this limited N may differ from actual ones. How well do texture measurements reproduce the actual distribution densities? The statistical relevance of such measurements is the main area of interest in the present paper.

In this article the *RP*-value is adopted as the value quantitatively characterizing this relevance. From this point of view the problem of evaluation of true distribution densities means the minimization of the *RP*-value over some variables. For evaluation of the pole density (for some PF), we consider the parameter of the measurement grid as the variable of the minimization problem. The number of grains N and the sharpness of the texture are the additional parameters of the problem.

Two approaches to solve the mentioned problem are proposed. One is the numerical simulation of the given distribution as the normal (Gaussian) distribution. The other is based on some estimation of the expected *RP*-value between the actual and experimental PFs.

It turns out that for the given type of the measurement grid (an equidistant grid) the optimal measurement grid parameter exists. This is one that minimizes the *RP*-value in dependence on the number of grains N in the sample and sharpness of the texture.

Keywords: Spherical singular integrals; Grain statistics; Normal distribution function

1. INTRODUCTION

Every experimental method of quantitative texture analysis (QTA) deals with samples which consist of some limited number of grains. In real samples this number can vary from hundreds to millions or even a larger

number of individual orientations. As a result, grain statistics is one of the most important causes of statistical errors that affect the measured data. The whole list of these causes also includes the grain-size statistics, neutron (electron) counting statistics, etc. This leads to the problem of pole (orientation) density estimation on the sphere S^2 (group $SO(3)$) with a constrained sample size. Some aspects of this problem were listed by Schaeben (1982) (see also references therein).

This paper is one more attempt to solve the mentioned problem on the sphere in a self-contained and easy-to-use form. In the general approach, different errors (grain statistics errors, grain-size statistics errors, approximation errors) depending on the external conditions (measurement grid, geometry of the experiment, the detector window width or the integral kernel) and the texture were taken into account (Sections 2–4). This approach was applied to the problem of optimal grid parameter estimation (Section 5) and to the problem of optimal smoothing (Luzin, 1997). This approach allows an extension for determination of other parameters in the optimal way, for example, the optimal measurement grid (optimal equidistributed pointset) on the sphere (cf. Cui *et al.*, 1995).

The advantage of the optimal measurement grid is apparent: the necessary measurement time is inversely proportional to the square of the grid step (further grid parameter). So a time-saving technique can be used, especially, in measurements of series of samples with close textures.

2. FUNDAMENTALS

The orientation distribution function (ODF) $f(g)$ is considered as the orientational density $(1/8\pi^2)f(g)$ on the rotational group $G \equiv SO(3)$ and the PFs $P_{h_i}(y)$ as the pole density $(1/4\pi)P_{h_i}(y)$ defined on the sphere S^2. The normalization properties are:

$$\frac{1}{8\pi^2}\int_G f(g)\,\mathrm{d}g = 1, \qquad \frac{1}{4\pi}\int_{S^2} P_{h_i}(y)\,\mathrm{d}\omega(y) = 1. \tag{1}$$

The fact is that the specimen measured in the texture experiment is obtained by sampling from the sample multitude with a true ODF $f^{\mathrm{t}}(g)$ and the PFs $P^{\mathrm{t}}_{h_i}(y)$. If the size of the specimen or the number of grains is N, then the specimen is described by the sampling ODF in

terms of δ-functions on $SO(3)$:

$$f^{s}(g,N)=\frac{1}{V}\sum_{n=1}^{N}V_{n}\delta(gg_{n}^{-1}),\quad V=\sum_{n=1}^{N}V_{n},\quad \frac{1}{8\pi^{2}}\int_{G}\delta(gg_{n}^{-1})\,\mathrm{d}g=1. \tag{2}$$

Also, for PFs we can write

$$P_{h_i}^{s}(\boldsymbol{y},N)=\frac{1}{V}\sum_{n=1}^{N}V_{n}\delta(\boldsymbol{y}-\boldsymbol{y}_{n}),\qquad \frac{1}{4\pi}\int_{S^{2}}\delta(\boldsymbol{y}-\boldsymbol{y}_{n})\,\mathrm{d}\omega(\boldsymbol{y})=1. \tag{3}$$

Mathematically, experimental PFs $P_{h_i}^{e}(\boldsymbol{y}_j,N)$ are

$$P_{h_i}^{e}(\boldsymbol{y}_j,N)=\int_{\Omega_j}P_{h_i}^{s}(\boldsymbol{y},N)K(\boldsymbol{y},\boldsymbol{y}_j,\{\rho\})\,\mathrm{d}\omega(\boldsymbol{y});$$
$$\boldsymbol{y}_j\in\Gamma;\ j=1,\ldots,J;\ J=\#\Gamma. \tag{4}$$

Here Γ is the predetermined measurement grid with $J=\#\Gamma$ points. $K(\boldsymbol{y},\boldsymbol{y}_j,\{\rho\})$ is the integral kernel for the jth point with the local support Ω_j (for more details see Schaeben, 1982; 1996). The dependence on $\boldsymbol{y}_j$ indicates that the integral kernels may differ from one another for different j. $\{\rho\}$ is the set of parameters for the kernel. $K(\boldsymbol{y},\boldsymbol{y}_j,\{\rho\})$, Γ, $\{\Omega_j\}$ are determined by the detector system and the geometry of the texture experiment. In the simplest case, $\{\Omega_j\}$ is a solid angle of the detector window for the jth points and

$$K(\boldsymbol{y},\boldsymbol{y}_j,\{\rho\})=\begin{cases}1/\|\Omega_j\|, & \boldsymbol{y}\in\Omega_j,\\ 0, & \boldsymbol{y}\notin\Omega_j,\end{cases} \tag{5}$$

when the detector has uniform sensitivity within the window.

In this paper, we adopt this simplest model of texture measurements. Moreover, we define the set $\{\Omega_j\}$ as a Dirichlet tessellation connected with an equidistant grid Γ:

$$\begin{aligned}\Gamma&=\{\boldsymbol{y}_j=(\theta_k,\varphi_l),\ j=(k,l)\}\\&=\begin{cases}\theta_k=k\Delta\theta,\ k=1,\ldots,N_1,\ \Delta\theta=\pi/N_1;\\ \varphi_l=l\Delta\varphi,\ l=1,\ldots,N_2,\ \Delta\varphi=2\pi/N_2;\end{cases}\end{aligned} \tag{6}$$

$$\Omega_j=\left\{\theta_k-\frac{\Delta\theta}{2}\le\theta<\theta_k+\frac{\Delta\theta}{2},\ \varphi_l-\frac{\Delta\varphi}{2}\le\varphi<\varphi_l+\frac{\Delta\varphi}{2}\right\};$$
$$j=1,\ldots,J;\ J=N_1N_2. \tag{7}$$

This simplest Dirichlet tessellation leads to the property

$$\int_{\{\Omega_j\}} d\omega(\boldsymbol{y}) = \sum_{j=1}^{J} \|\Omega_j\| = 4\pi, \tag{8}$$

which, usually, is not fulfilled in the real experiment.

The main aim of the texture measurement is to evaluate the true pole densities $P^{\mathrm{t}}_{h_i}(\boldsymbol{y})$ by experimental PFs $P^{\mathrm{e}}_{h_i}(\boldsymbol{y}_j, N)$ defined at the points $\boldsymbol{y}_j \in \Gamma$. Quantitatively, this means that one needs to minimize some function which is the integral measure of expected errors

$$R = somefunction\Big(E\Big\{|P^{\mathrm{t}}_{h_i}(\boldsymbol{y}_j) - P^{\mathrm{e}}_{h_i}(\boldsymbol{y}_j, N)|\Big\}\Big), \quad \boldsymbol{y}_j \in \Gamma. \tag{9}$$

In this paper we are trying to solve this. We find the optimal value $\Delta\theta = \Delta\varphi$ for an equidistant grid Γ with $\{\Omega_j\}$ and $K(\cdots)$ as described above when the number of grains N is the parameter. As the R-value, we take the function analogous to RP-value

$$RP(\varepsilon, P^{\mathrm{t}}_{h_i}(\boldsymbol{y}_j), P^{\mathrm{e}}_{h_i}(\boldsymbol{y}_j, N)) = \frac{1}{J}\sum_{j=1}^{J}\left|\frac{P^{\mathrm{t}}_{h_i}(\boldsymbol{y}_j) - P^{\mathrm{e}}_{h_i}(\boldsymbol{y}_j, N)}{P^{\mathrm{t}}_{h_i}(\boldsymbol{y}_j)}\right|,$$
$$\boldsymbol{y}_j \in \Gamma, \ j = 0, \ldots, J; \ J = \#\Gamma. \tag{10}$$

Conventional summing is performed with the sensitivity level $\varepsilon = 0.1$.

Now we discuss two approaches to this problem.

3. SIMULATION WITH GAUSSIAN DISTRIBUTION

It is well known that the orientation

$$g = [\omega, \boldsymbol{n}] = [\omega, \vartheta, \varphi], \quad g \in SO(3),$$
$$0 \le \omega < 2\pi, \ 0 \le \vartheta \le \pi, \ 0 \le \varphi \le 2\pi, \tag{11}$$

can be presented as a point on the unit hypersphere S^3 in the four-dimensional Euclidean space $\Re^4$ with hyperspherical coordinates

$$(r, \psi, \vartheta, \varphi) \equiv (\psi, \vartheta, \varphi), \quad r = 1, \ 0 \le \psi \le \pi, \tag{12}$$

where $2\psi=\omega$. The Euclidean coordinates of this point are $\boldsymbol{r}=(x_1, x_2, x_3, x_4)$,

$$\boldsymbol{r} \in S^3 \subset \Re^4, \qquad \sum_{i=1}^{4} x_i^2 = 1. \tag{13}$$

Now consider a sequence of t rotations through a fixed angle Λ about a randomly oriented axis with random direction. Let $\rho_t(\boldsymbol{r})$ be the distribution density after t steps have been passed. Following Roberts *et al.* (1984) define the Brownian motion law as

$$\rho_t(\boldsymbol{r}') = \langle \rho_{t-1}(\boldsymbol{r}) \rangle, \quad \boldsymbol{r}', \boldsymbol{r} \in S^3. \tag{14}$$

The operator $\langle \cdots \rangle$ implies the averaging of the function defined on S^3 over the two-dimensional sphere with the center $\boldsymbol{r}'$ and the radius $\Lambda/2$. It is easy to obtain the solution of the characteristic equation

$$\langle \phi_\lambda \rangle = \lambda \phi_\lambda, \tag{15}$$

where ϕ_λ is the characteristic function and λ is the characteristic value.

Namely, only zonal harmonics of order l in terms of Gegenbauer polynomials C_l^1,

$$\phi_l = \frac{C_l^1(\cos(\omega/2))}{C_l^1(1)} = \frac{1}{l+1} C_l^1\left(\cos\frac{\omega}{2}\right) = \frac{\sin((l+1)\omega/2)}{(l+1)\sin(\omega/2)}, \tag{16}$$

provide the nonzero solution of (15) with the eigenvalues

$$\lambda_l = \frac{1}{l+1} C_l^1\left(\cos\frac{\Lambda}{2}\right) = \frac{\sin((l+1)\Lambda/2)}{(l+1)\sin(\Lambda/2)} \tag{17}$$

due to the property of zonal harmonics to be constant on the sphere $S^2 = SO(3)/SO(2)$. Tesseral harmonics satisfy (15) as well: each side of (17) vanishes. So the surface hyperspherical harmonic Z_l of order l (a linear combination of zonal and tesseral harmonics) with a $(l+1)^2$-fold degeneracy is the averaging operator eigenfunction corresponding to the eigenvalue defined by (17).

So, if the initial distribution density is a certain orientation $g=[0,0,0]$, $g \in SO(3)$ or

$$\rho_0(\boldsymbol{r}) = \sum_{l=0}^{\infty} Z_l(\boldsymbol{r}), \quad \boldsymbol{r} = \left(\frac{\omega}{2}, \vartheta, \varphi\right) \in S^3, \tag{18}$$

then we obtain

$$\rho_1(\boldsymbol{r}) = \sum_{l=0}^{\infty} \lambda_l Z_l(\boldsymbol{r}), \tag{19}$$

$$\vdots$$

$$\rho_t(\boldsymbol{r}) = \sum_{l=0}^{\infty} \lambda_l^t Z_l(\boldsymbol{r}) = \frac{1}{4\pi^2} \sum_{l=0}^{\infty} (l+1)^2 \left[\frac{\sin((l+1)\Lambda/2)}{(l+1)\sin(\Lambda/2)}\right]^t \frac{\sin((l+1)\omega/2)}{(l+1)\sin(\omega/2)}. \tag{20}$$

One can readily see that in the limit $t \to \infty$ when Λ is fixed, $[\cdots]^t \to 0$ for all $l \neq 0$ and uniform distribution takes place

$$\rho(\boldsymbol{r}) = \frac{1}{4\pi^2}. \tag{21}$$

In special convergence conditions $t \to \infty$, $\Lambda \to 0$, $\Lambda^2 t \to const$ we get

$$\rho(\boldsymbol{r}) = \frac{1}{4\pi^2} \sum_{l=0}^{\infty} (l+1) \exp\left\{-l(l+2)\left(\frac{\Lambda}{2}\right)^2 \frac{t}{3!}\right\} \frac{\sin((l+1)\omega/2)}{\sin(\omega/2)}. \tag{22}$$

The requirement

$$\rho\left(2\pi - \frac{\omega}{2}, \pi - \vartheta, \varphi \pm \pi\right) = \rho\left(\frac{\omega}{2}, \vartheta, \varphi\right), \tag{23}$$

which is valid for the orientational space, leads to the symmetry of $\rho(\boldsymbol{r})$ on S^3:

$$\rho(\boldsymbol{r}) = \rho(-\boldsymbol{r}), \quad \boldsymbol{r} \in S^3 \subset \Re^4, \tag{24}$$

or to omitting of all odd terms in (8):

$$\rho(\boldsymbol{r}) = \frac{1}{2\pi^2} \sum_{l=0}^{\infty} (2l+1) \exp\{-l(l+1)D\} \frac{\sin((2l+1)\omega/2)}{\sin(\omega/2)}, \quad D = \frac{\Lambda^2 t}{6}. \tag{25}$$

This distribution was also derived by Savyolova (1984) in terms of infinitely divisible distributions. Following Savyolova (1984), the corresponding distribution on the sphere $S^2 \subset \Re^3$ can be written as

$$\rho(y) = \frac{1}{4\pi}\sum_{l=0}^{\infty}(2l+1)\exp\{-l(l+1)D\}P_l(\cos\beta), \quad y = (\beta,\varphi) \in S^2, \tag{26}$$

where $P_l(\cos\omega)$ are the Legendre polynomials.

For application, small finite values $\Lambda \ll 1$ and $t \gg 1$ can be taken to produce numerically the circular limit distribution (25) with the parameter $D = \Lambda^2 t/6$. To do this one needs to set the initial orientation and then, subject it to a series of rotations through a fixed angle Λ around the random axis in the following way:

$$\vartheta_n = \arccos(2a_n - 1), \quad \varphi_n = 2\pi_n \cdot b_n, \quad 0 \le \vartheta_n \le \pi, \quad 0 \le \varphi_n < \pi, \tag{27}$$

where $a_n, b_n \in [0, 1]$ are the random numbers.

N independent numerical experiments produce some specific sampling OBF in the form (2), where N is the number of "grains". Using the projection formula the corresponding PFs $P^{s}_{h_i}(y, N)$ can be calculated. If the grid $\Gamma = \{y_j\}$ and the integral kernel $K(y, y_j, \{\rho\})$ are predetermined the experimental PF $P^{e}_{h_i}(y_j, N)$ can be calculated. Because the exact distributions $f^{t}(g)$ and $P^{t}_{h_i}(y)$ in the form (25) and (26) are known, the corresponding R-value can be easily calculated. The R-value allows us to make the following estimation using the mean value:

$$\bar{R}_1 \approx \frac{1}{M}\sum_{m=1}^{M} RP(\varepsilon, P^{t}_{h_i}(y_j), P^{e,m}_{h_i}(y_j, N)), \tag{28}$$

where $P^{e,m}_{h_i}(y_j, N)$ is the mth independent realization of the simulated experimental PF $P^{e}_{h_i}(y_j, N)$. In the presented examples, $M = 10$ was used.

In Fig. 1 these mean RP-values are shown by circles on the dependence of the equidistant grid parameter for $N = 500$ and $N = 5000$. For these numerical experiments a simple texture model with only one

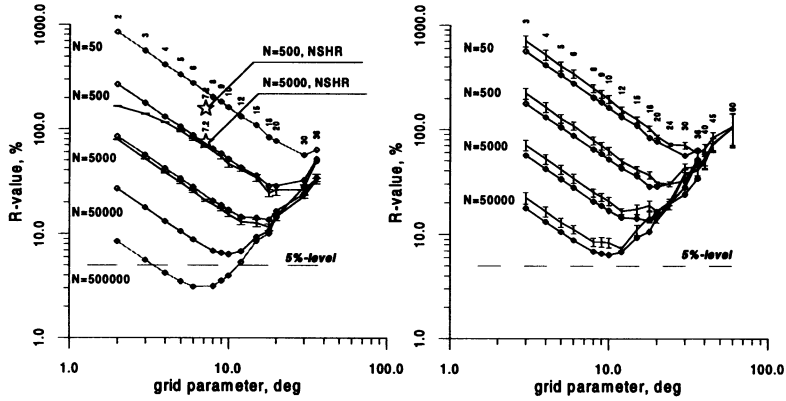

FIGURE 1 The dependence of the R-value on the grid parameter for different numbers of grains. Left: lines with the error-bars are the $R1$-estimates, lines with the signs are the $R2$-estimates. The $R1$-estimates for the real experimental conditions of the NSHR-spectrometer are shown by stars. Right: lines with the signs are the $R2$-estimates, lines with the error-bars are the $R2$-estimates averaged over 100 random mesorientations of the texture component and the measurement coordinate system.

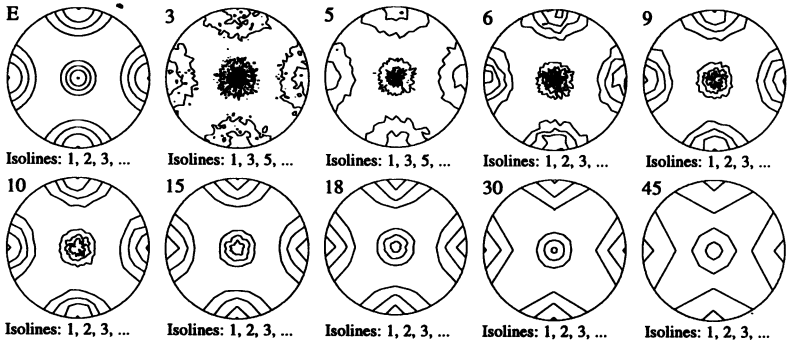

FIGURE 2 Examples of the pole figures {100} "measured" on different grids. The grid parameters are shown on the top left of the pole figure. The label "E" is for the exact pole figure. $N = 5000$.

Gaussian component was chosen. The center of Gaussian is $g = \{0, 0, 0\}$. The width parameter $D \approx 0.042$ was determined using $t = 400$ and $\Lambda = 0.025$. This corresponds to HWHM of the component $\approx 19.7°$. The examples of PFs with this texture are shown in Fig. 2.

4. ESTIMATION OF THE *R*-VALUE

Another approach is based on the *R*-value estimates (9). From (3)–(5), it follows that

$$P^{e}_{h_i}(y_j, N) = \int_{\Omega_j} P^{s}_{h_i}(y, N) K(y, y_j, \{\rho\})\, d\omega(y)$$
$$= \frac{1}{V}\frac{1}{\|\Omega_j\|}\int_{\Omega_j}\sum_{n=1}^{N} V_n \delta(y - y_n)\, d\omega(y)$$
$$= \frac{4\pi}{\|\Omega_j\|}\frac{\sum_{y_n\in\Omega_j} V_n}{V} = \frac{4\pi}{\|\Omega_j\|}\frac{n_j}{N} \equiv \frac{4\pi}{\|\Omega_j\|} w_j(N). \qquad (29)$$

Here, we take a model of material with equal grains ($V_n = V_0$, $V = NV_0$) to exclude the effect of grain-size statistics from the consideration. (In the case when the grains are distributed in accordance with some grain size distribution with the parameter V_0 (the center of distribution) and the parameter ΔV^2 (dispersion of distribution), an additional term proportional to the $\Delta V/V_0$ appears in the previous equation). The quantity n_j is a random variable and means the number of grains with poles $y_n \in \Omega_j$. Let us also introduce the integrated true PFs defined at the points of the grid $y_j \in \Gamma$:

$$P^{i}_{h_i}(y_j) = \int_{\Omega_j} P^{t}_{h_i}(y) K(y, y_n, \{\rho\})\, d\omega(y)$$
$$= \frac{1}{\|\Omega_j\|}\int_{\Omega_j} P^{t}_{h_i}(y)\, d\omega(y) \equiv \frac{4\pi}{\|\Omega_j\|} p_j, \qquad (30)$$

where $p_j = \text{Prob}\{y \in \Omega_j\}$.

So the *R*-value can be estimated as

$$R = \frac{1}{J'}\sum_{j=1}^{J'}\sqrt{E\left\{\left(\frac{P^{t}_{h_i}(y_j) - P^{e}_{h_i}(y_j, N)}{P^{t}_{h_i}(y_j)}\right)^2\right\}}$$
$$\approx \frac{1}{J'}\sum_{j=1}^{J'}\left\{\frac{(P^{t}_{h_i}(y_j) - P^{i}_{h_i}(y_j))^2}{(P^{t}_{h_i}(y_j))^2} + \frac{E\{(p_j - w_j)^2\}}{p_j^2}\right.$$
$$\left. + 2\frac{(P^{t}_{h_i}(y_j) - P^{i}_{h_i}(y_j))}{P^{t}_{h_i}(y_j)}\frac{E\{(p_j - w_j)\}}{p_j}\right\}^{1/2}. \qquad (31)$$

The first term depends only on the true distribution and its integrals and reflects the goodness of the approximation with singular integrals. Due to the fact that for Bernoulli trials with N events,

$$\begin{aligned} E\{n_j\} &= Np_j;\ D\{n_j\} = Np_j(1-p_j); \\ E\{w_j\} &= p_j;\ D\{w_j\} = p_j(1-p_j)/N, \end{aligned} \tag{32}$$

the third term vanishes and the second can be further evaluated:

$$\frac{E\{(w_j-p_j)^2\}}{p_j^2} = \frac{D\{w_j\}}{p_j^2} = \frac{1}{N}\frac{1-p_j}{p_j}. \tag{33}$$

Finally, we obtain the R-value estimate,

$$\bar{R}_2 = \frac{1}{J'}\sum_{j=1}^{J'}\sqrt{\left[\int_{\Omega_j}\left(1-\frac{P_{h_i}^{t}(y)}{P_{h_i}^{t}(y_j)}\right)\mathrm{d}\omega(y)\right]^2+\frac{1}{N}\frac{1-p_j}{p_j}}. \tag{34}$$

To illustrate the numerical results, the same texture model as in the previous case was taken. The results are also presented in Fig. 1 to enable quantitative comparison of the two approaches. As it can be seen, the second approach gives us a sufficiently good estimate. It should be noted that the second approach is a more time-saving one.

5. OPTIMIZATION OF MEASUREMENT GRID: RESULTS

The obtained estimates give us the possibility of investigating some problems connected with the accuracy of PFs measured in texture experiment. The following problems can be solved.

1. Let the texture sharpness be specified (at least approximately) and the number of grains be evaluated in the investigated specimen. From these data the optimal measurement grid parameter can be determined.
2. For the given measurement of grid parameter and estimated sharpness of the texture, the necessary number of grains in the investigated specimen can be indicated to achieve the prescribed level of the expected R-value (Fig. 3).

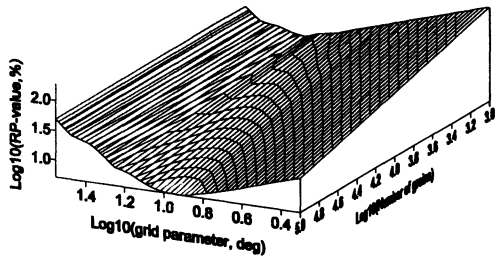

FIGURE 3 The dependence of the R-value on the number of grains and the grid parameter plotted as a surface.

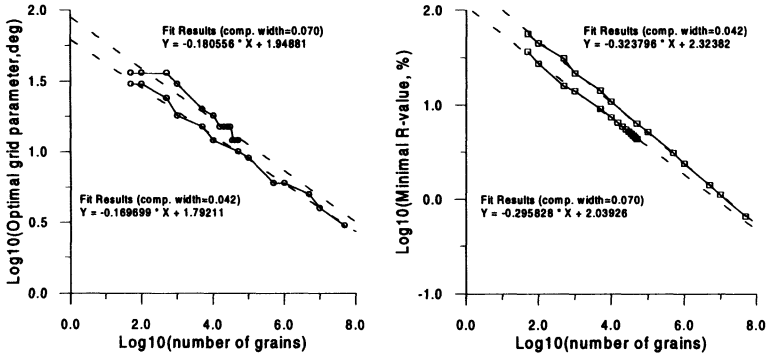

FIGURE 4 The dependence of the optimal grid parameter and the corresponding minimal $R2$-value on the number of grains on the double-logarithmic scale. Both curves can be linearly approximated.

3. If the measurement grid is prescribed and the number of grains is known, the upper limit of the sharpness can be determined. Measurements of specimens with a sharper texture lead to loss of information (or smoothing of the texture data).

The first problem is the focus of our attention. It turns out that the measurement grid parameter and the minimal R-value which corresponds to this optimal parameter depend, in the simplest way, on the number of grains. The results for textures with two different sharpnesses are presented in Fig. 4. This figure quantitatively describes the evident behavior of the R-value when the number of grains changes. The following rule is quantitatively confirmed: the only way to enhance the accuracy of measured PFs is to increase the number of grains in

the sample. These also provide quantitative support for the rule: the sharper the texture the finer must the grid be; but in spite of the fine grid the accuracy of the measured PFs is worse than for a less sharp texture.

6. CONCLUSION

In this paper, the influence of grain statistics on the accuracy of PFs measured in the texture experiment was investigated. Two approaches to quantitative analysis of errors related to the number of grains in the investigated sample were proposed. So, the main regularities of grain statistics are established. The problem of optimal measurement grid is solved. Although the question whether or not the optimal measurement grid is also optimal for the ODF reproduction yet needs to be answered, it is proved that optimal measurement grid is useful for the problems required only PFs. However, there are some hints that the optimal measurement grid is really useful for ODF reproduction (Luzin, 1997).

Moreover, the main idea of this paper allows extension to different objects which come from the ODF (e.g. properties averaged with texture). List of possible applications is here.

- It is possible to investigate the statistical relevance of ODF just in the same way as it was done for PFs. This is, especially, applicable in the OIM-method. It should be noted that the results obtained for PFs cannot be directly extended to the ODF. For example, the optimal measurement grid for PFs needs not be optimal for the grid of ODF.
- Also, the tolerance of different ODF reproduction methods can be established since the error bounds for ODF and PFs can be simultaneously determined.
- The other possible application is comparison of material properties of samples with poor grain statistics. It should be of particular assistance in the strain measurements when the small gauge volume is the principal feature of the experiment.
- Both approaches allow taking into consideration grain-size statistics. In the first approach, it is necessary to append the distribution over the grain size (volume). In the second approach, an additional term appears in (34).

Acknowledgment

The author would like to thank Dr. D. Nikolayev for helpful discussions.

References

Bunge, H.J. (1996). *Proc. of Workshop "Math. Methods of Texture Analysis", Textures and Microstructures* **25**, 71–108.
Cui, J. and Freeden, W. (1995). AGTM-Report Nr. 142, University Kaiserslautern.
Luzin, V. (1997). (these proceedings).
Roberts, P.H. and Winch, D.E. (1984). *Adv. Appl. Prob.* **16**, 638–655.
Savyolova, T.I. (1984). *Zavodskaya Laboratoriya* **50**, 48–52 (in Russian).
Schaeben, H. (1982). *Math. Geology* **14**(3), 205–216.
Schaeben, H. (1996). *Proc. of Workshop "Math. Methods of Texture Analysis", Textures and Microstructures* **25**, 159–169.